



Cellular metabolism network of *Bacillus thuringiensis* related to erythromycin stress and degradation



Pulin Zhou^a, Ya Chen^a, Qiyang Lu^b, Huaming Qin^a, Huase Ou^a, Baoyan He^a, Jinshao Ye^{a,*}

^a School of Environment, Guangdong Key Laboratory of Environmental Pollution and Health, Jinan University, Guangzhou 510632, Guangdong, China

^b College of Biology and Food Engineering, Guangdong University of Education, Guangzhou 510303, Guangdong, China

ARTICLE INFO

Keywords:

Antibiotics
Degradation
Proteomics
Fatty acids
Macrolide

ABSTRACT

Erythromycin is one of the most widely used macrolide antibiotics. To present a system-level understanding of erythromycin stress and degradation, proteome, phospholipids and membrane potentials were investigated after the erythromycin degradation. *Bacillus thuringiensis* could effectively remove 77% and degrade 53% of 1 μM erythromycin within 24 h. The 36 up-regulated and 22 down-regulated proteins were mainly involved in spore germination, chaperone and nucleic acid binding. Up-regulated ribose-phosphate pyrophosphokinase and ribosomal proteins confirmed that the synthesis of protein, DNA and RNA were enhanced after the erythromycin degradation. The reaction network of glycolysis/gluconeogenesis was activated, whereas, the activity of spore germination was decreased. The increased synthesis of phospholipids, especially, palmitoleic acid and oleic acid, altered the membrane permeability for erythromycin transport. Ribose-phosphate pyrophosphokinase and palmitoleic acid could be biomarkers to reflect erythromycin exposure. Lipids, disease, pyruvate metabolism and citrate cycle in human cells could be the target pathways influenced by erythromycin. The findings presented novel insights to the interaction among erythromycin stress, protein interaction and metabolism network, and provided a useful protocol for investigating cellular metabolism responses under pollutant stress.

1. Introduction

Antibiotics have a strong market demand as medicines used in the treatment and prevention of bacterial infections. Owing to inappropriate use or abuse of antibiotics, partial microbes conduct evolutionary processes to acquire antibacterial-resistance genes, triggering the emergence of resistance to antibiotics. Some molecular mechanisms related to the resistance have been mentioned. For example, acquired resistance derives from a mutation in a chromosome or the acquisition from exotic DNA in other species (Haaber et al., 2016). The spread of antibacterial resistance often occurs in the environments where are frequently under the stresses of antibiotics through mutations or horizontal gene transfer (Penesyan et al., 2015). Cross-resistance to antibiotics with similar structure may also occur when antibiotics or bactericides are abused (Fleitas and Franco, 2016). The ineffective therapy results in antibiotics accumulation and emission in environment leading to harmful effects.

Erythromycin, as one of the most widely used macrolide antibiotics, is produced by a strain of *Streptomyces erythreus*. It can

inhibit protein synthesis through its binding to ribosomal proteins (Cetecioglu et al., 2015; Siibak et al., 2009). Currently, bacterial resistance has caused the extensive concern for the erythromycin abuse. In general, erythromycin resistance is mediated by efflux pump proteins, ribosomal methylase and modifying enzymes. Drug efflux pumps and CYPs have been found jointly adjust bioavailability of macrolides, causing reduced drug intake and failed treatment (Pal and Mitra, 2006). For example, erythromycin can be excreted out of cells through the regulation of MsrA in *staphylococci* (Reynolds et al., 2003). In *Streptococcus pneumoniae* CP1000, a lower-level erythromycin resistance is resulted in mutations clustered in the carbon terminus (Canu et al., 2002). A L22 protein RplV is considered to be a functional molecule related to macrolide resistance in various bacteria (Cagliero et al., 2006). A ribosomal RNA methylase ErmB in *Campylobacter coli* ZC113 is responsible for high-level macrolide resistance (Qin et al., 2014). Two members of erythromycin esterase superfamily, EreA and EreB, have been confirmed inactivating erythromycin (Qin et al., 2014). The ATP binding cassette transporters and ComD are the key proteins for erythromycin uptake in quorum-sensing (Zhao et al., 2015).

* Corresponding author.

E-mail address: folaye@126.com (J. Ye).

To alleviate their negative impacts and develop metabolic approaches for the biological control of antibiotics, their biodegradation were studied. The previous investigations found that erythromycin A could be degraded by *Ochrobactrum* sp. WX-J1 with the production of four intermediates, including 3-depyranosyloxy erythromycin A, 7, 12-dihydroxy-6-deoxyerythronolide B, 6-deoxyerythronolide B and propionaldehyde (Zhang et al., 2017). With $1.8 \mu\text{g mL}^{-1}$ esterase treatment for 16 h, the degradation efficiency of erythromycin at $100 \mu\text{g mL}^{-1}$ reached to 52% (Llorca et al., 2015).

These previous reported mechanisms at biomolecular level related to the resistance, transport and transformation of antibiotics are investigated based on the functions of individual target genes or proteins (Blair et al., 2015). To present a global understanding, omics technologies are the insightful approaches to clarify the cellular metabolism network associated with antibiotic resistance and biodegradation. The isobaric tag for relative and absolute quantitation (iTRAQ) technology for proteome identification, characterization and quantification is one of those mentioned approaches to clarify the system-level understanding of erythromycin resistance and biotransformation. The results would provide basic evidence associated with the metabolic network of target species under antibiotics stresses.

Bacillus thuringiensis GIMCC1.817 could serve as an efficient strain for erythromycin degrading. It is a gram-positive bacterium producing insecticidal proteins commonly used as biological pesticides. It is also a functional microbe for the degradation of pollutants, such as dimethyl phthalate (Brar et al., 2009), fipronil (Mandal et al., 2013) and triphenyltin (Wang et al., 2017). Investigating the relationship between antibiotic degradation and proteome expression can reveal the key scientific mechanisms related to the synergetic control of insects and pollutants. That is why this species was selected as a model microbe in the current study. Proteome, phospholipids, membrane characteristics and carbon substrate metabolism were studied after the erythromycin degradation. Some target biomolecules reported in the previous researches and differentially expressed proteins found in the current study were analyzed in the reactome database (<http://www.reactome.org/>) to predict metabolic impact of erythromycin on human cells.

2. Methods

2.1. Strain and chemicals

Bacillus thuringiensis GIMCC1.817 was an effective strain selected by our group for the degradation of multiple pollutants (Tang et al., 2016) and was stored at the Microbiology Culture Centre of Guangdong Province, China.

Erythromycin was purchased from Sigma Aldrich (St. Louis, MO, USA), which was dissolved in chromatography grade methanol. Trypsin (Promega, V5280, USA) and iTRAQ reagent multiplex kit (Sigma, PN 4352135, USA) were used in this experiment. The common broth medium for cells culture contained 3 g L^{-1} beef extract, 10 g L^{-1} peptone and 5 g L^{-1} NaCl. The composition of mineral salt medium (MSM) for erythromycin exposure was 30 mg L^{-1} KH_2PO_4 , 20 mg L^{-1} NaCl, 30 mg L^{-1} NH_4Cl and 10 mg L^{-1} MgSO_4 , respectively.

2.2. Microbial culture and erythromycin degradation

B. thuringiensis was inoculated into the MSM at 100 r min^{-1} on a rotary shaker for 6–96 h. Subsequently, cells were separated from the medium by centrifugation at 6000 r min^{-1} for 10 min and then washed three times using sterile phosphate buffer solution (pH 7.4).

Twenty milliliter MSM with $0.1\text{--}3.0 \text{ g L}^{-1}$ cells and $1 \mu\text{M}$ erythromycin were inoculated into 20 mL MSM in the dark at 30°C on a rotary shaker at 100 r min^{-1} . After treatment for 24 h, residual erythromycin in the resultant supernatant was detected to determine the removal efficiency, and the total erythromycin in the supernatant and cells was used to determine the degradation efficiency.

2.3. Erythromycin analysis

The quantitative analysis of erythromycin was performed using a high performance liquid chromatography with a tandem mass spectrometer (HPLC/MS², TripleQuad 5500, Applied Biosystems SCIEX, USA) (Perez et al., 2017). The detailed analysis procedure is presented in Text S1.

2.4. Genome sequencing, assembly, and annotations

Cells were sent to Sangon Biotech (Shanghai, China) for high-throughput sequencing of paired-end and mate-pair in the Illumina HiSeq. 2000 platform. Quality control of the raw data was performed after sequencing detection. High-quality bases (Phred score, > 20) were reserved as valid data, and a total of 10,000 reads were randomly selected from the high-quality data to the nt database for comparison. High-quality bases obtained from paired-end and mate-pair sequencing were 2,378,013,607 bp and 1,243,334,169 bp without obvious pollution. *De novo* assembly and annotations were analyzed by SPAdes and RAST, respectively. GapCloser and GapFiller software were selected to close gaps from the raw scaffolds obtained from SPAdes software.

2.5. Proteomics analysis

After the erythromycin treatment, cells were separated and washed using phosphate buffer solution for protein extraction (Text S2). The control samples without erythromycin were also treated in the same condition. The extracted proteins were digested (Text S3), labeled and desalinated (Text S4), respectively. After dryness in a vacuum concentrator, the samples were resolved with solution (2% v/v ACN, 0.1% v/v formic acid), centrifuged at $12,000 \text{ r min}^{-1}$ for 20 min, and detected by an AB Sciex Triple TOF 5600 mass spectrometer (AB Sciex, Framingham, MA, USA) equipped with a Nanospray III source (AB Sciex). LC-MS-MS data were analyzed with Protein Pilot software (4.5 version, AB SCIEX, Foster City, USA) and matched the database with following criteria: significance threshold $p < 0.05$ (with 95% confidence) and ion score or expected cut-off less than 0.05 (with 95% confidence). Peptides from the control samples and erythromycin-degraded samples were labeled by tag 114 and 115, respectively. A protein with concentration alteration ($115:114$) ≥ 1.2 or ≤ 0.83 was considered to be differentially up or down expressed.

2.6. Phospholipids detection

Phospholipids were analyzed according to a reference (Yang et al., 2017) by gas chromatograph tandem mass spectrometer (SHIMADZU GCMS-QP 2010 Ultra) with a DB-5MS ($30 \text{ m} \times 0.25 \text{ mm} \times 0.25 \mu\text{m}$) quartz capillary column. The scanning range of mass spectrometer and electron energy of electron ionization were 50–500 m/z and 70 eV, respectively. The column temperature was set to 140°C for 2 min, then, heated to 260°C with 3°C per minute. The sample inlet temperature and ion source temperature were 250°C and 230°C , respectively. Peak area and internal standard curve method were used for quantification.

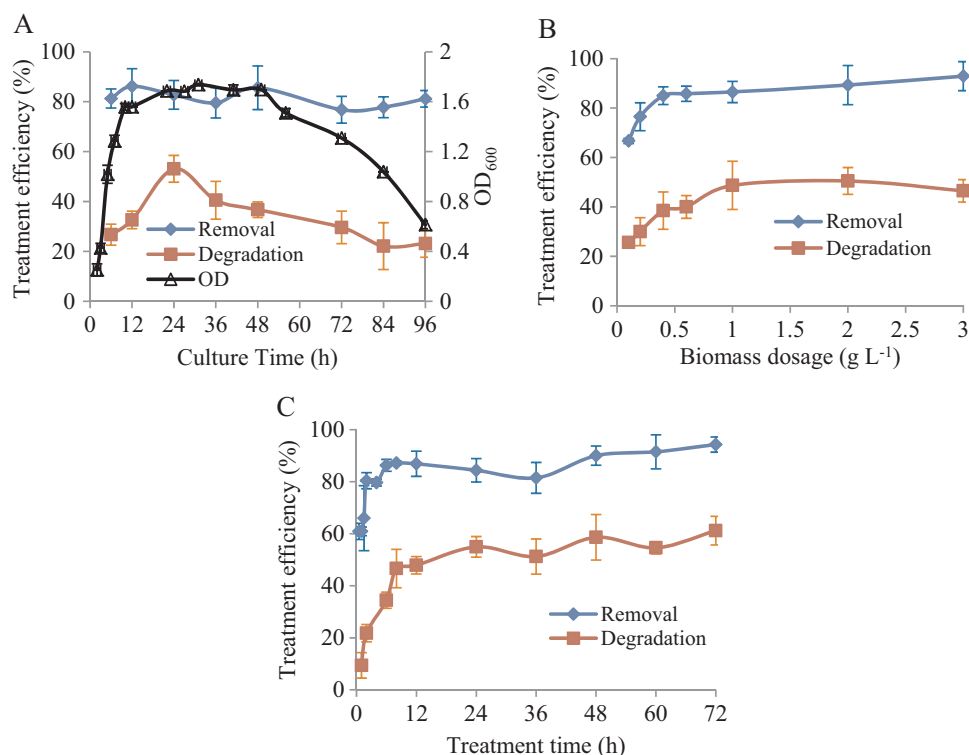


Fig. 1. (A) Effect of cellular culture time on degradation of erythromycin at 1 µM by 1 g L⁻¹ cell for 24 h; (B) Degradation of erythromycin at 1 µM by 0.1–3 g L⁻¹ cell for 24 h; (C) Degradation of erythromycin at 1 µM by 1 g L⁻¹ cell for 0.5–72 h.

2.7. Membrane potential analysis

Membrane potential analysis was conducted according to the previous study (Wang et al., 2017). Briefly, cells were collected and suspended in 200 µL of JC-1 dye solution followed by incubation at 25 °C for 15 min in a dark place. Subsequently, cells were analyzed by a FACSaria flow cytometer (BD, USA). The JC-1 monomers emitted green fluorescence, while the aggregates emitted red fluorescence. These two kinds of fluorescence were captured through 527 and 590 nm long-pass filters, respectively.

3. Results and discussion

3.1. Erythromycin degradation

The optical density of cells in the culture medium at different culture times was detected to determine bacterial growth phases. Fig. 1A illustrated that there was almost no lag phase, inferring that *B. thuringiensis* adapted to the culture medium in a short time. After cells grew exponentially between 2 and 12 h, a stable phase between 12 and 48 h was followed by an apoptotic phase. To confirm the optimal time points to harvest cells for erythromycin degradation, cells cultured for different time were separated from the culture medium and were used to degrade erythromycin.

The removal efficiency was determined by the decrease in concentration of erythromycin in the treatment solution. It included metabolic degradation, surface adsorption and intracellular accumulation. In Fig. 1A, the relative stable curve of the removal ranging from 77% to 86% implied that the erythromycin removal was not primarily depended on cellular metabolism, whereas, the

degradation up to 53% was relied on the phases of cellular growth. Cells with the optimal activity of erythromycin degradation harvested at 24 h were therefore used in the following experiments. It was reported that erythromycin biodegradation was fast with 50% removal within 13 h by the enriched activated sludge culture (Terzic et al., 2018) and 97% degradation by an *Ochrobactrum* sp. after 72 h (Zhang et al., 2017). Safety assessment of the residual erythromycin and its products were studied by performing bacterial density and toxic effects on algae. The results showed low growth inhibition and less toxicity after erythromycin degradation for a certain period of time (Terzic et al., 2018).

Both curves of the removal and degradation after erythromycin treatment by different dosages of biomass for 24 h and erythromycin treatment at different time showed initial increasing tendencies followed by stable phases (Figs. 1B and 1C). The degradation contributed approximately 50% of erythromycin removal meant that there were still half of removed pollutant adsorbed or accumulated by cells (Fig. 1B). Initially, the removal efficiency was far more significant than degradation (Fig. 1C). Subsequently, the degradation efficiency continued to increase to 55% at 24 h, narrowing the gap between removal and degradation. This finding suggested that the removal process was initially dominated by biosorption, and degradation gradually increased the contribution of erythromycin removal.

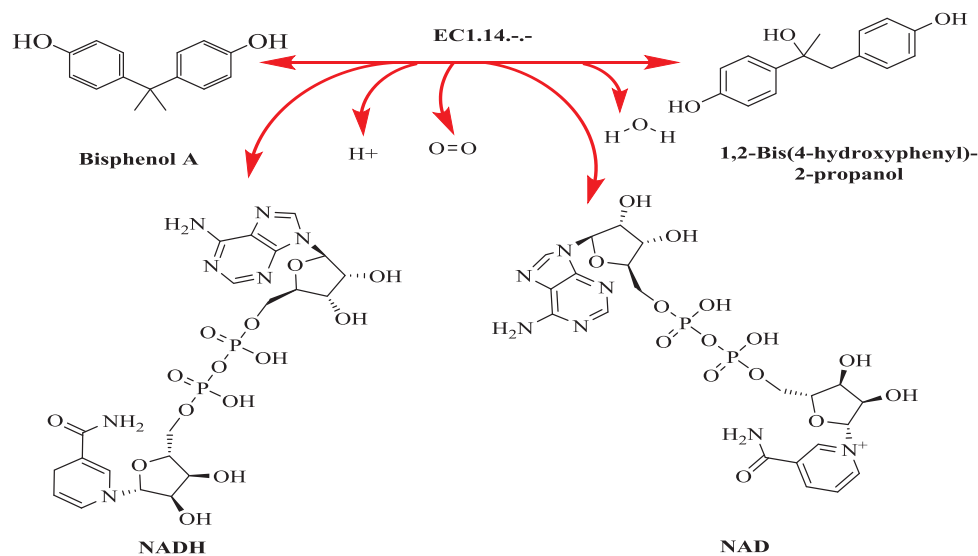
3.2. Predicted genes and identified proteins classification

To reveal the functional genes related to erythromycin degradation, the cellular genome was analyzed. It consisted of 5,713,790 base pairs with an average GC content of 34.86%.

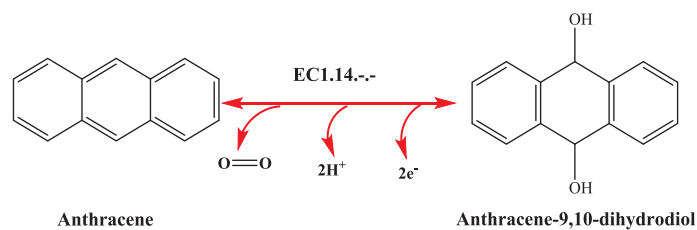
Protein-coding sequences, GC content and GC skew were depicted in Fig. 2A. GO function classification of genes was mainly clustered in cellular process and metabolic process, cell and cell part, binding and catalytic activity (Fig. 2B).

To reveal whether there were some genes related to pollutant degradation or metabolism, the reactions catalyzed by the encoded proteins were mapped in the KEGG metabolic network (Fig. S1). Some

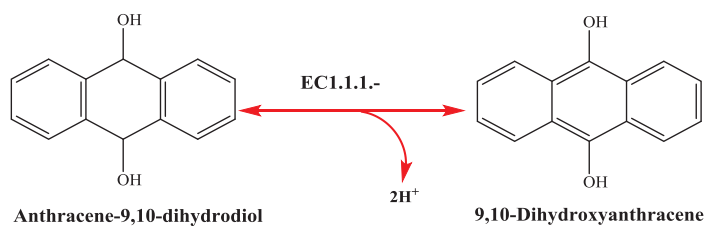
functional genes in *B. thuringiensis* were found enriched in metabolic pathways, such as drug metabolism by other enzymes, and xenobiotics and drug metabolism by cytochrome P450s. Among these metabolic reactions, oxidoreductases catalyze bisphenol A to 1, 2-bis (4-hydroxyphenyl)-2-propanol (Eq. (1)). Anthracene can be transformed to anthracene-9, 10-dihydrodiol and 9, 10-Dihydroxyanthracene (Eqs. (2) and (3)) by catalysis of oxidoreductases and alcohol dehydrogenase, respectively.



(1)



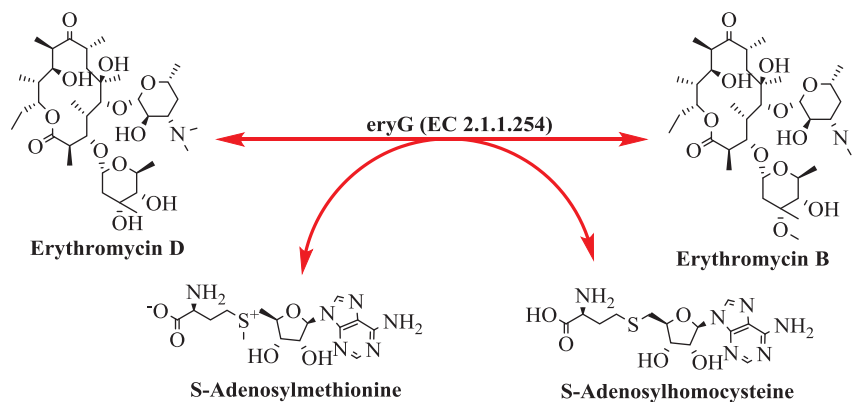
(2)



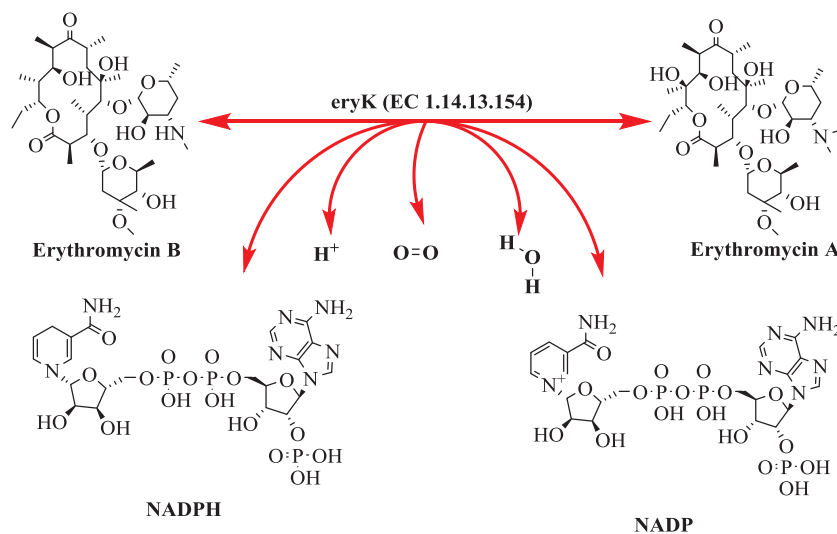
(3)

P450 expressed in *B. thuringiensis* was involved in triphenyltin degradation through splitting a carbon-tin bond, generating a phenol and a diphenyltin, which would further be transformed to monophenyltin and tin (Wang et al., 2017; Yi et al., 2017). Triphenyltin has been used extensively as algicides and molluscicides in antifouling products for decades. With the similar function as triphenyltin, erythromycin is supposed to be transformed by the same pathway. Erythromycin served as a substrate of CYP 3A4 is an evidence for this inference (Carls et al., 2014). CYPs are also the enzymes catalyzing the process of erythromycin synthesis and transformation (Eqs. (4) and (5)). One of CYPs, EryG methylates the precursor erythromycin D, forming erythromycin B, which is then converted to the most active form of erythromycin (erythromycin A).

from the control and treatment groups were compared. The significantly different expression of 58 proteins, 36 up-regulated and 22 down-regulated proteins were induced after erythromycin degradation (Table S1). As shown in Fig. 2C, the molecular functions of these proteins involved were catalytic activity (35.4%), structural molecule activity (31.3%), binding (27.1%), transporter activity (4.2%) and translation regulator activity (2.1%). In Fig. 2D, the biological processes were related to metabolic process (46.2%), cellular process (38.5%), cellular component organization or biogenesis (7.7%), localization (8.8%), biological regulation (1.9%), response to stimulus (1.9%). Most of the proteins played a role of catalytic activity to regulate the cellular metabolic process. The proteins involved in the cell-



(4)



(5)

Peptide methionine sulfoxide reductase MsrA (EC 1.8.4.11) and macrolide efflux protein (EC 2.7.7.2) were reported to be erythromycin resistance proteins in *Enterococcus faecalis* (Chouchani et al., 2012). The genes encoding these proteins and an esterase (EC 3.1.1.1) were found in *B. thuringiensis* through the genome analysis. This finding inferred that *B. thuringiensis* used in the current study can be a functional strain for erythromycin degradation. The results of some key influence factors related to the erythromycin degradation were the direct evidence of this inference (Figs. 1A and 1C).

To demonstrate the relationship between erythromycin degradation and cellular metabolism network of *B. thuringiensis*, proteome of cells

lular process were mainly ribosomal proteins, which could bind with RNA for translation regulation to mediate protein synthesis. The protein directly related to response to stimulus was identified as chaperone protein DnaK, which was essential to strengthen the microorganisms against external stress, such as heat, acid and cold stresses, antibiotic treatment (Chiappori et al., 2015; Jiao et al., 2015). Cold shock-like protein CspD was overexpressed in the treatment group. Up-regulated cold shock proteins can increase bacterial adaptation to external stress, not just cold stimulation (Keto-Timonen et al., 2016). It seemed that CspD could enhance the adaptability of *B. thuringiensis* under

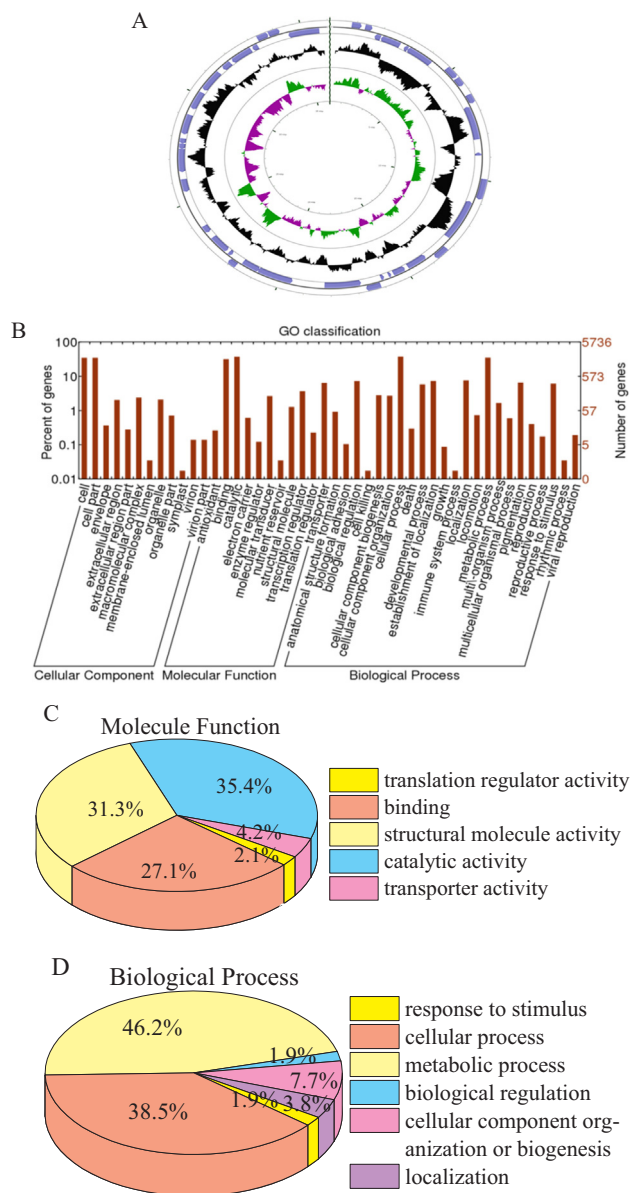


Fig. 2. (A) Features of the circular map were as followed. (1) Forward-strand protein-coding sequences (blue), (2) Reverse-strand protein-coding sequences (blue), (3) GC content (black), (outer of the circle indicates higher GC content than the average of whole genome, and the inner indicates less GC content than the average of whole genome), (4) GC skew (green stands for positive GC skew; violet represents negative GC skew), (5) Genome scale; (B) Biological function of *Bacillus thuringiensis* genome; (C) Molecular function of identified differentially expressed proteins through Gene Ontology (GO) classification; (D) Biological process of identified differentially expressed proteins through Gene Ontology (GO) classification. (For interpretation of the references to color in this figure legend, the reader is referred to the web version of this article.)

erythromycin or other substances stress, and it would facilitate the degradation of erythromycin.

3.3. Spore proteins and chaperone proteins

An endospore is a dormant and non-reproductive structure produced by certain bacteria. It can be activated to the vegetative state at a

favorable environment. In this germination process, spore germination proteins served as a germinant receptor for identifying germination agent (Paredes-Sabja et al., 2011). In the current result, a spore germination protein GerE, a transcription factor, connected with the sporulation process (Errington, 2003; McKenney et al., 2013) was dramatically decreased in concentration. The different expression of this protein led to spore phenotype diversity (Sturm and Dworkin, 2015). Stage IV sporulation protein SpoIVA was a spore coat protein assembled into the basement layer of the coat, with the use of energy from ATP hydrolysis (Kim et al., 2006; Ramamurthi and Losick, 2008). SpoIVA can affect the localization of SpoVM and the synthesis of peptidoglycan. Down-regulation of this protein inferred the inhibition of peptidoglycan synthesis, thereby inhibiting the growth of the cells.

GrpE and chaperone protein DnaK associated with the process of protein synthesis, transport, folding and degradation were the co-expression proteins with slightly down regulation (Fig. 3). They involved in protein disaggregation (Doyle et al., 2015) were linked to down-regulated leucine-tRNA ligase LeuS and serine-tRNA ligase SerS (Fig. 3). GrpE promoted the circulation of DnaK between ATP-DnaK and ADP-DnaK. This seemed to be detrimental for cells to resist the adverse environment, whereas, other overproduced proteins could alleviate the adverse effects induced by down-regulated chaperone proteins (Zhang et al., 2016).

3.4. Metabolic pathways analysis

The metabolic network, including amino acid metabolism, the glycolysis/gluconeogenesis pathway, citrate cycle and pentose phosphate pathway, catalyzed by the differentially expressed proteins was shown in Fig. 4.

For amino acid metabolism, L-lysine 2, 3-aminomutase KamA, cryptic catabolic NAD-specific glutamate dehydrogenase GudB and arginase RocF were up-regulated, whereas, SerS and LeuS were down-regulated. KamA is an enzyme in lysine degradation pathway, catalyzing the conversion of the L-lysine to L-β-lysine, which will further transform to 3, 5-diaminohexanoate, 5-amino-3-oxohexanoic acid, L-3-aminobutyryl-CoA, crotonoyl-CoA, acetoacetyl-CoA and acetyl-CoA, successively. Its over-expression meant the increased production of acetyl-CoA. Acetyl-coenzyme A synthetase AcsA catalyzes the inter-conversion of acetate and acetyl-CoA through a two-step reaction. It was down-regulated, resulting in the decrease in the transformation of acetyl-CoA to acetate, which further triggered the accumulation of acetyl-CoA.

GudB converts glutamate to α-ketoglutarate, producing ammonium as a byproduct. Normally, GudB will be up regulated at starvation to increase the production of α-ketoglutarate, which can be catalyzed in the citrate cycle with ATP generation. RocF is the final enzyme in the urea cycle converting arginine to ornithine and urea. These three increased proteins facilitated the production of acetyl-CoA, which participates in various biosynthetic pathways, and acts as a signal of growth and proliferation (Cai et al., 2011; Song et al., 2016). That is why the concentrations of phospholipids C16:1ω7 and C16:0 were increased (Fig. 7A).

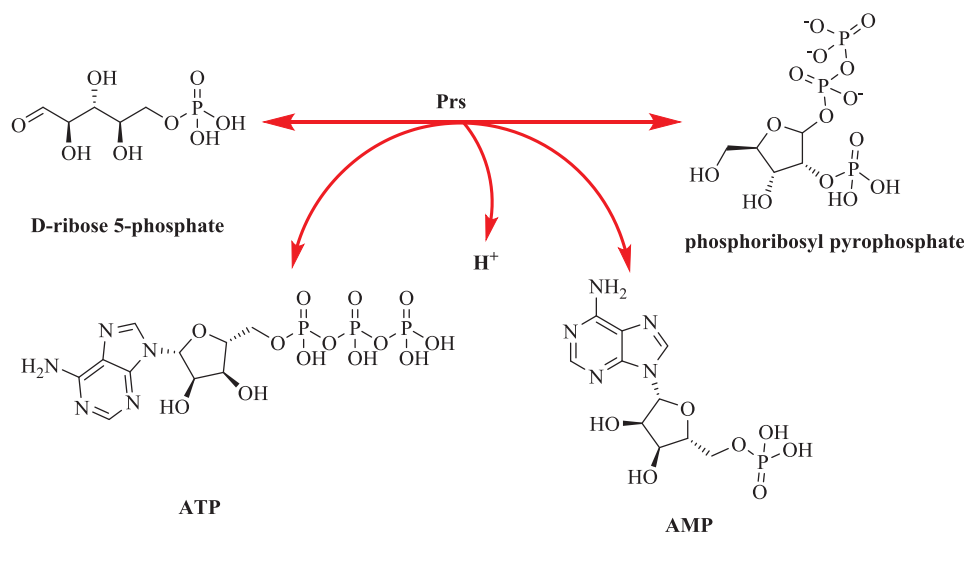
Regarding carbohydrate metabolism, the differentially expressed proteins were involved in glycolysis/gluconeogenesis, citrate cycle and pentose phosphate pathway. Among these proteins, fructose-bisphosphate aldolase FbaA is a glycolytic enzyme catalyzing a reversible reaction that converts the aldol and fructose 1, 6-bisphosphate into the triose phosphates dihydroxyacetone phosphate and glyceraldehyde 3-phosphate, which occurs as an intermediate in pentose phosphate pathway, fructose and mannose metabolism and glycolysis/gluconeogenesis. Glyceraldehyde-3-phosphate dehydrogenase 1 Gap1 catalyzes glyceraldehyde-3-phosphate to 1, 3-bisphosphoglycerate with NAD⁺

reduction into NADH. The synergetic up-regulated biosynthesis of FbaA and Gap1 confirmed that the glycolysis/gluconeogenesis pathway was significantly enhanced during the exposure to erythromycin, whereas, pentose phosphate pathway, and fructose and mannose metabolism might be depressed due to the transformation of glyceraldehyde 3-phosphate to 1, 3-bisphosphoglycerate. The up-regulated expression of Gap1 was also consistent with the inference that the concentration or activity of Gap1 would be enhanced in response to stresses (Roland et al., 2014). Lactate dehydrogenase found in nearly all living cells can be used as a model enzyme for biochemical adaptation. Lactate dehydrogenase 3 Ldh3 converts the reversible reaction of pyruvate to lactate with concomitant interconversion of NADH and NAD⁺. Its enhanced expression combined with the above findings confirmed that the chemical reaction network of glycolysis/gluconeogenesis pathway and pyruvate metabolism was activated in response to erythromycin degradation.

The pyruvate dehydrogenase complex PdhC is composed of three enzymes, pyruvate decarboxylase (E1), dihydrolipoyllysine acetyltransferase (E2) and dihydrolipoyl dehydrogenase (E3). PdhC links glycolysis/gluconeogenesis metabolism to citrate cycle due to its function of producing acetyl-CoA. AcsA initially combines acetate with ATP to form acetyl-adenylate followed by the transfer of the acetyl

biosynthesis of nucleotides, lipids and amino acids. Transketolase Tkt catalyzes the reversible transfer of a two-carbon ketol group from a ketose donor to an aldose acceptor in this pathway. The analysis of its molecular function in the KEGG metabolism database revealed that Tkt in *B. thuringiensis* catalyzes the reaction between beta-D-fructose 6-phosphate and D-xylulose 5-phosphate. Therefore, its down-regulation resulted in the low synthesis of ATP, CoA and NAD(P)⁺ (Jung et al., 2015), and the suppression of glycolysis and pentose phosphate pathway.

Ribose-phosphate pyrophosphokinase Prs, belonging to the ribose-phosphate pyrophosphokinase family, catalyzes D-ribose 5-phosphate to the phosphoribosyl pyrophosphate (PRPP) with ATP consumption (Eq. (6)). In this process, Mg²⁺ is used as the activating cation (Hove-Jensen and McGuire, 2004). PRPP is the key node metabolite for the synthesis of RNA and DNA, and the metabolism of purine, pyrimidine and pyridine nucleotides (Hove-Jensen et al., 2017). The increase of Prs suggested an enhanced transport of Mg²⁺, and an increase in the production of PRPP, which then up-regulated the synthesis of RNA, inferring that erythromycin accelerated DNA transcription of *B. thuringiensis*. This finding was further confirmed by the up-regulated expression of 20 ribosomal proteins in the current study. Therefore, Prs can be a biomarker to reflect erythromycin toxicity.



group from acetyl-adenylate to the sulfhydryl group of CoA, producing acetyl-CoA. In the current study, PdhC and AcsA were down-expressed, resulting in the reduction of acetyl-CoA transformation through this by-pathway, whereas, the up-regulated pyruvate metabolism is the main pathway for acetyl-CoA generation, ensuring the enhanced synthesis of this compound. Acetyl-CoA further delivers the acetyl group to the citrate cycle to be oxidized for the production of energy and some low molecular organic acids, such as succinate. The up-regulated expression of succinyl-CoA ligase [ADP-forming] subunit beta SucC catalyzing succinyl-CoA to succinate with energy production is the direct evidence of acetyl-CoA transformation. Except acetyl group transfer, acetyl-CoA participates in many biochemical reactions in lipid and amino acid metabolism, which could be certified by the different synthesis of serine, leucine, arginine, lysine, glutamate, ornithine and phospholipids in the current study.

The pentose phosphate pathway provides the precursors for the

Among these fourteen 50S subunit proteins and six 30S subunit proteins, most of them had close relationship with Prs. Some previous studies reported that most antibiotics affected the normal cellular metabolism by inhibiting energy generation (Liu et al., 2014; Lobritz et al., 2015). Overexpression of ribosomal proteins in the current study facilitated protein synthesis and energy generation for antibiotic resistance and transformation. One of the significantly up-regulated proteins, 50S ribosomal protein L22 RplV related to macrolide resistance (Fyfe et al., 2016) was chosen for phylogenetic tree analysis to determine whether it could be a biomarker to reflect erythromycin stress. The phylogenetic relationship (Fig. 5) suggested that RplV of *B. thuringiensis* has the same function as other bacteria, such as *Staphylococcus aureus* and *Staphylococcus haemolyticus*, with homology up to 73.2% and 74.1%. It can be assumed that the up-regulated Prs and ribosomal proteins, enhanced the synthesis of bacterial protein, DNA and RNA for resistance to erythromycin stress.

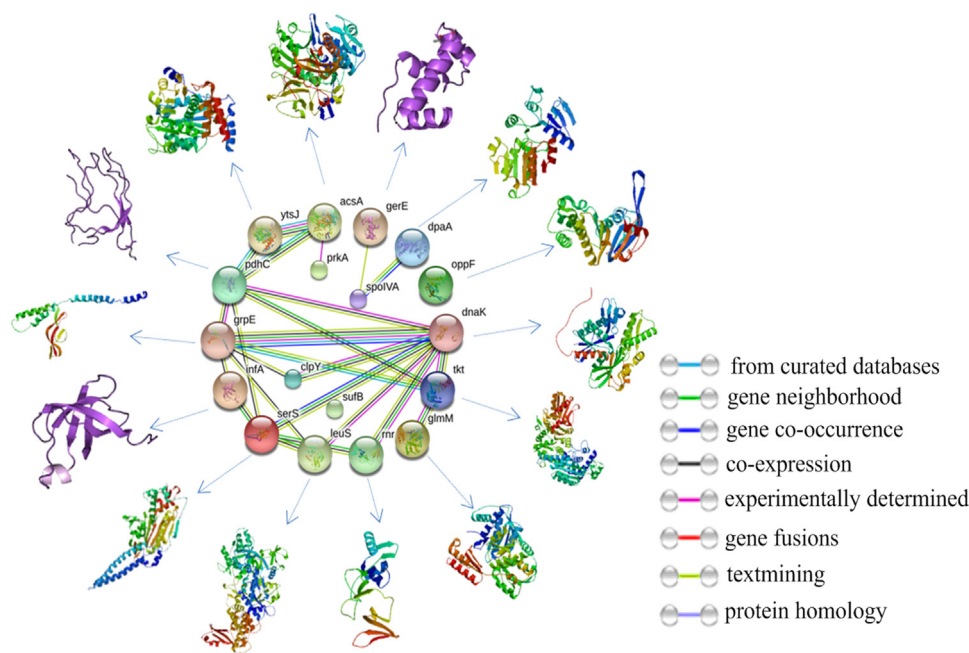


Fig. 3. The interaction of 17 down-regulated proteins.

3.5. Potential target metabolic pathways affected by erythromycin on human cells

To predict whether the exposure and degradation of erythromycin conduct similar metabolic impacts on human cells, some biomarkers reported in the previous researches and differentially expressed proteins found in the current study were analyzed in the reactome database (Fig. 6A). Among these 74 proteins, 48 of them were involved in glycerophospholipid biosynthesis, phospholipid metabolism and phosphatidic acid synthesis (Fig. 6B, Table S3). CYP4F11 can relieve the mitochondrial fatty acid β -oxidation damage by regulating the oxidation of 3-hydroxy fatty acids (Dhar et al., 2008). In the presence of cholesterol, the catalytic domain of a membrane-anchored protein CYP3A4 and its position in the lipid membrane were altered (Navratilova et al., 2015). Both CYP4F11 and CYP3A4 were related to lipid metabolism. The alteration of their expression and position in membrane directly influence the substrate uptake in cells. As an inhibitor of CYP3A4, erythromycin decreased lignocaine clearance (Orlando et al., 2003). The phosphatidic acid worked with other proteins, regulate the activity of enzymes, including Type I phosphatidylinositol 4-phosphate 5-kinase, to adapt to different environments (Cockcroft, 2009). In the process of erythromycin therapy, the phosphatidic acid synthesis might be altered in human cells. The change in phosphatidic acid concentration resulted in the alteration of enzyme activity, which further regulated cellular adaptability.

In disease pathway, the Hsp90 co-chaperone CDC37 was involved in signaling. The level of this protein was reported higher in human breast cancer tissues, and it could act as a new target protein for the disease diagnosis or therapy (Kim et al., 2014). The same function protein of CDC37 in *B. thuringiensis* was the DnaK, which was down regulated for the toxicity of erythromycin. When patients were treated with erythromycin, CDC37 is worth our attention for it was the target proteins of erythromycin therapy or resistance.

In the pyruvate metabolism and citrate cycle, the L-lactate dehydrogenase and succinate-coA ligase were marked in Fig. 6C. Upregulated lactate dehydrogenase could serve as a significant marker in predicting patients with organ or tissue damages caused by arsenic (Karim et al., 2010). Succinate-coA ligase caused a reduced mitochondria DNA content in blood samples of the patients with mitochondrial DNA depletion syndromes (MDDSs) (Dimmock et al., 2010). Increased L-lactate dehydrogenase activity in epithelial cells after exposed to e-cigarette vapor, induced cell damage, which might cause oral infections (Rouabhia et al., 2017). The amino acid sequence alignment of these two proteins (EC 1.1.1.27, EC 6.2.1.5) in *B. thuringiensis* and Homo sapiens were showed in Fig. 6D with the identity of 34.8%, 46.8%, and the similarity of 71.5%, 77.7%. These findings inferred that when treated with erythromycin, these two proteins might also be differentially regulated in human cells.

3.6. Expression of phospholipids and changes of membrane potential

Alteration of phospholipid synthesis directly changes the cellular membrane mobility, which can affect the signal transmission and a series of metabolic activities in cell. It was reported that *Enterococci* resisted to daptomycin by decreasing the C18:1 ω 7c phospholipid, increasing rigidity of cell membrane (Mishra et al., 2012). In this experiment, seven phospholipids (Fig. 7A), myristic acid (C14:0), pentadecanoic acid (C15:0), palmitoleic acid (C16:1 ω 7), palmitic acid (C16:0), linoleic/linoleic acid (C18:2 ω 6), oleic acid (C18:1 ω 9c) and stearic acid (C18:0) were detected. Among them, palmitoleic acid and palmitic acid increased remarkably. Palmitoleic acid is a biomarker to reflect environment stress. For example, changes in lipid metabolism, especially palmitoleic acid up-regulation, were intended to modulate the homeostasis of retinal pigmented epithelial cells under 4-hydroxynonenal stress (Gutierrez et al., 2016). The increase of unsaturated fatty acids, enhanced membrane permeability to some degree,

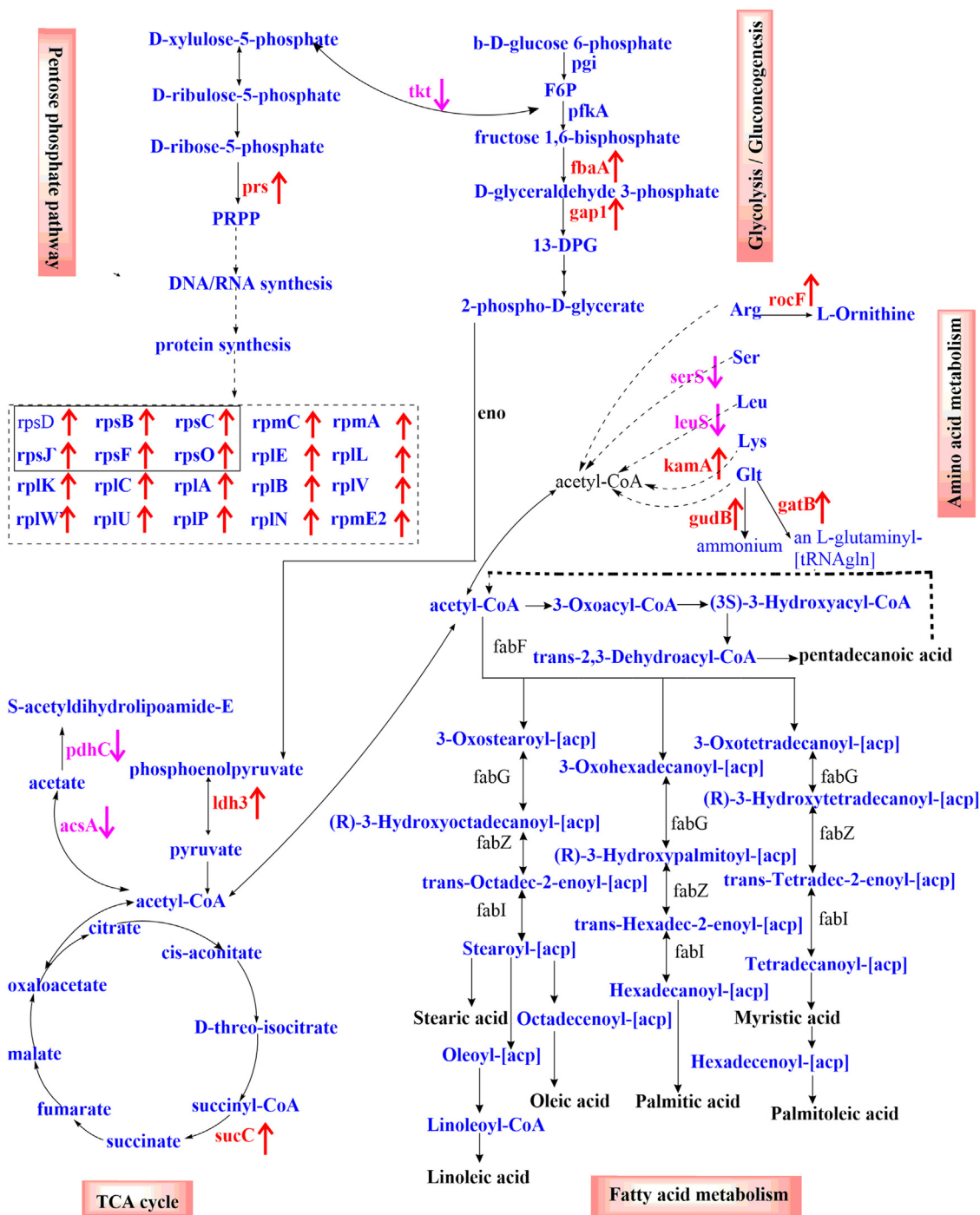


Fig. 4. Metabolic network of cells in response to erythromycin stress. Up-regulated proteins were shown in red marker. Down-regulated proteins were shown in violet marker. (For interpretation of the references to color in this figure legend, the reader is referred to the web version of this article.)

facilitating the exchange of ions between the inside and outside of cellular membrane. The transport of erythromycin as a carbon source might also be accelerated.

The synthesis of fatty acids consumes ATP, NADPH and a large amount of acetyl-CoA, which are primarily generated through the glycolytic pathway and the pentose phosphate pathway. In this

experiment the over-expressed proteins FbaA, Gap1 and Prs accelerated the metabolism of the above pathways. Although enoyl-[acyl-carrier-protein] reductase [NADH] FabI associated with fatty acid synthesis remained no significant change, the total amount of fatty acids detected as well as the proportion of unsaturated fatty acids to saturated fatty acids increased. This phenomenon was primarily due to an increase in

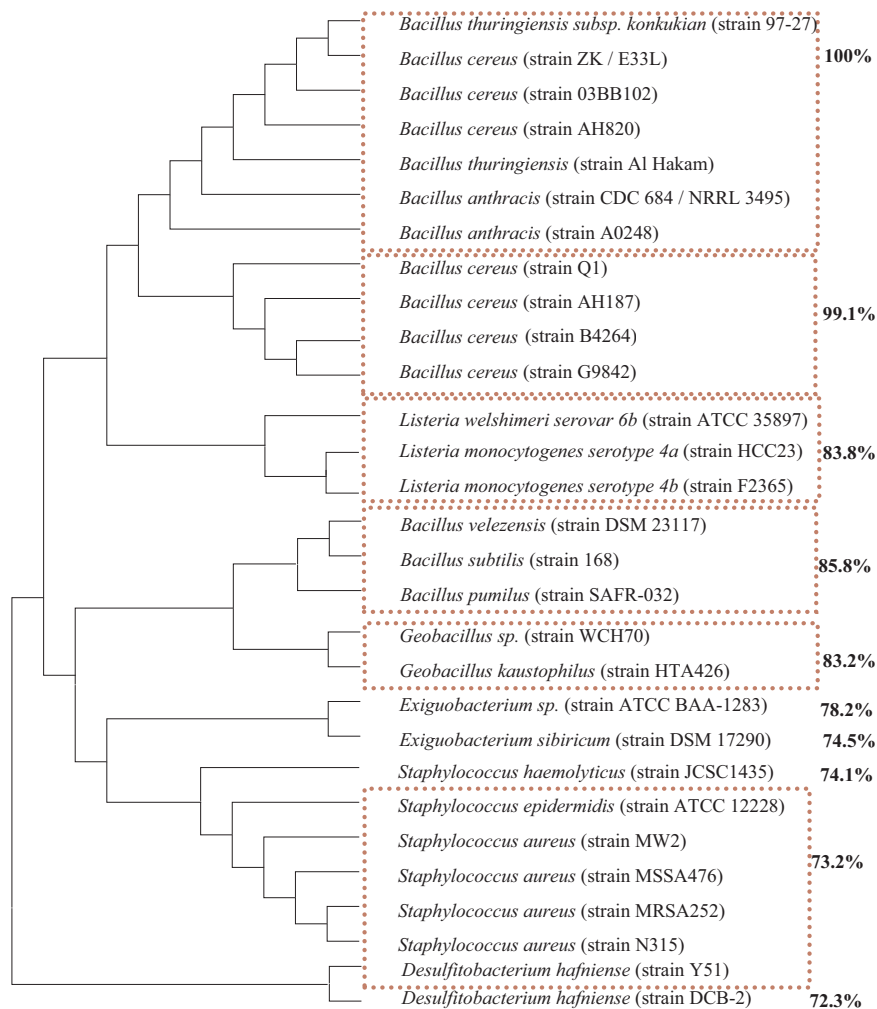


Fig. 5. Phylogenetic relationship of species contained rplV.

3-oxoacyl-[acyl-carrier-protein] synthase II FabF, 3-oxoacyl-(acyl-carrier-protein) reductase FabG, and beta-hydroxyacyl-[acyl carrier protein] dehydratase FabZ (Fig. 7B, Table S4) which were directly regulated fatty acid synthesis.

The changes of membrane potential can influence the distribution of specific proteins which are associated with cell division, thus affect the growth of bacteria (Strahl and Hamoen, 2010). After incubation for 5 h, the cell membrane potential was increased in both the control and degradation groups compared with that of 0 h (Fig. S2), and this might be caused by a replacement of MSM culture.

The membrane potential of the treatment samples at 12, 18 and 24 h kept the same level with 0 h (Fig. S2). Compared with the control, the membrane potential of the treatment samples had no significantly changes at 0, 5, 12, 18 h (Fig. S2). It showed that the toxicity of erythromycin on cell membrane potential was limited.

4. Conclusions

After the degradation of erythromycin at 1 μ M for 24 h, the removal and degradation efficiencies were up to 77% and 53%, and 36 and 22 proteins were up-and down-regulated, respectively. These proteins altered amino acid metabolism, citrate cycle, glycolysis/gluconeogenesis, and pentose phosphate pathway in *B. thuringiensis*. The synthesis of proteins, DNA and RNA were facilitated by the over-expressed Prs and 20 ribosomal proteins. The prediction of erythromycin influence on *Homo sapiens* presented insight into drug metabolism in human cells. Membrane potential detection results were consistent with the results of phospholipids, indicating increased cell membrane permeability. The Prs and palmitoleic acid could be biomarkers to reflect erythromycin toxicity.

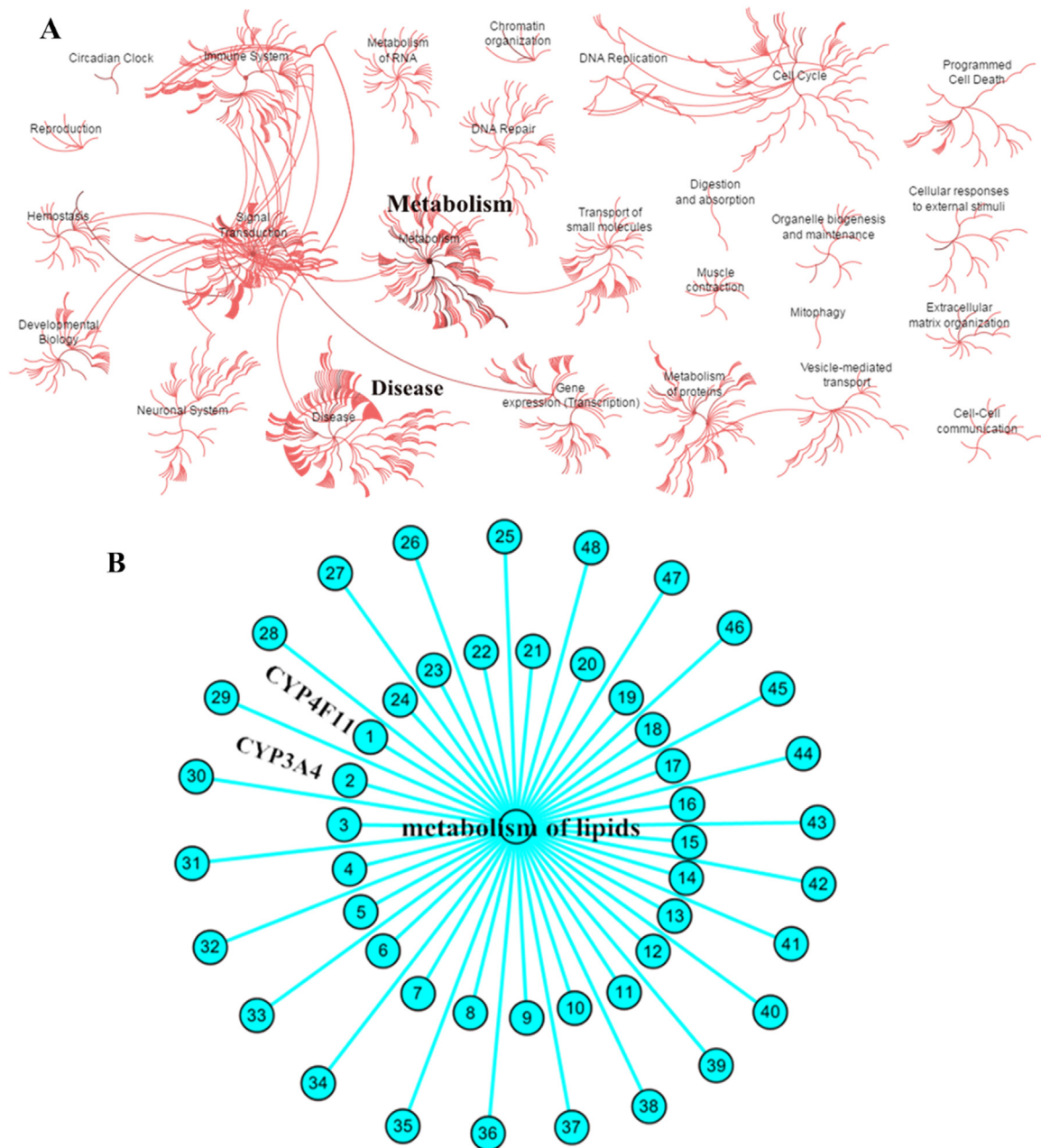
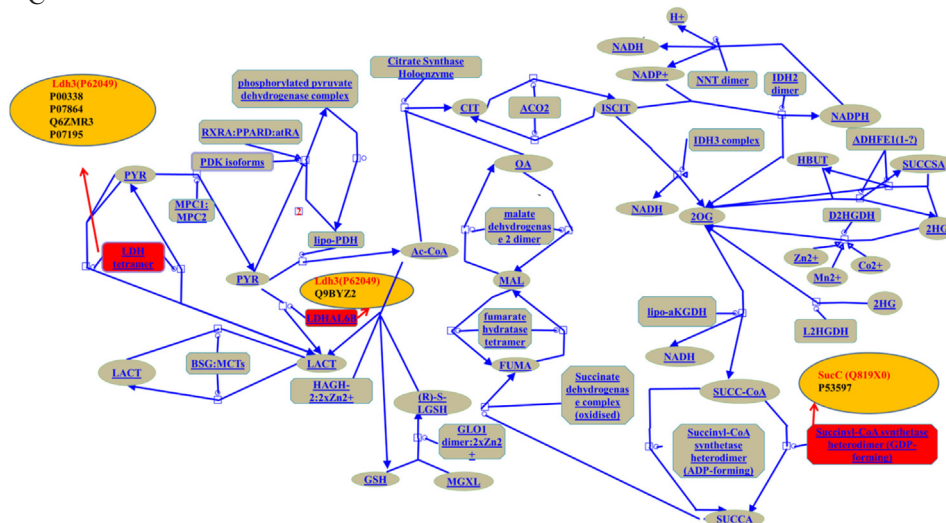


Fig. 6. (A) The related pathways in reactome pathway database; (B) 48 proteins involved in lipids metabolism, the detailed explanation of the numbers were illustrated in attachment; (C) Amino acid sequence alignment of DnaK and CDC37, Ldh3 and LDHAL6, SucC and SUCLA2; (D) The pyruvate metabolism and citrate cycle regulated by the target functional proteins related to erythromycin treatment.

C



D

Ldh3	*****
LDHAL6	BMSWTVVVRASQRVSSVGNFLCLGMALCPRQATRIPLNGTWLFTPVSKMATVKSELIER
Ldh3	***MKRNTRKIAITGTLVSSCAYSIVNQGICEHLLIDINHERAVGHEAMDLSHCINP
LDHAL6	FTSEKPVVHHSKYSITGTSVGMACAISILLKGLSDELAVDLDEDKLKGITMDLQHGSPF
Ldh3	TNTRTKVYAGSYEDCKDMDIVITAGPAPKPGQSRDLTLGASAKIMESVVGVMESGFDG
LDHAL6	TKMPNIVCSKDYFVANSNLVITAGARQEKGETRLNLVQRNVALFKLMISSIVQVSPHC
Ldh3	IFLLASNPVDIITYQVWKLSPNRRVIGTGTSLDSSRLRTLSEMLHVDPRSIIHGYSLG
LDHAL6	KLIVSNPVDILTYVWKLSPNRRVIGSGCNLDARFRFLIGQKLGTHSESCHGWILG
Ldh3	EHGDSQMVAVSHVTVGKPLQLLEKQDFCELDLDEIVEKTAKAGWEIYKRKGTYYG
LDHAL6	EHGDSVPVWGVNITAGVPLKDLNSDICTDKDPEQWKNVHKEVTATAYEITKMKGYTSA
Ldh3	IGNSLAVIASSIFNDYRVIAVSAILDGEYGEY*DLCTGVPALITRDGIREIYELNLTED
LDHAL6	IGLSVADITESTLKNLRRIRPVSTIIKGLYGIDEEVFLSIPCLIGENGTNLIKRILTFE
Ldh3	EESRFAKSNIDILRDYMKTIQY
LDHAL6	EEAHLKKSAKTLVETQNKLL
SucC	*****MNIHEYQG
SUCLA2	MAAMFYGRVAVATLRNHRPRTAQRAAAQVLGSSGLFNNHGLVQQQQRNLSLHEYMS
SucC	KAVLRSYCVSYENGVKVAFTVEEAVEAARELGTDVCEKAQHAGGRGK*****AGGVK
SUCLA2	MELLQEAQVSYFKGVAKSPDEAYAIANKLGSKIVVKAQVLAGGRGKGTFSGLKGGVK
SucC	YAKNLDVVRTYAESILGTTLVTHQTGPEGKEYKRLLEEGCDIKKEYVYGLVLDRAITSQV
SUCLA2	IVFSPPEEAKAVSSMI GKGLFTKQTGEKGRICNQLVCEKYPREYFYAITMERSFQGP
SucC	VLMASEEGGTELEFYAEKTPKELFKKEYIDPAVGLQGFQARRIAFNINIPKELVGVQAVKFM
SUCLA2	VLIGSSHGGVNIEDYAAESPEALIKPEIDIEEGIKKEQALQAQKMGFPNIVESAANM
SucC	MGLYRAFTEKDCSTAEINPLYTTGEGKYMALDAKLNFDNVALYRHKDILELRLDEEDSK
SUCLA2	VKLYSLFLKYDAITIEINPMVEDSDGAVLMDAKINFDNSAYRQKKIFDLQDWTFQEDER
SucC	EIEASKYDLNYPIDGNIGCMVNGAGLAMA TMDLIKHYHGDPANFLDVGGGATAEKVTEA
SUCLA2	DKDAAKANLNYIGLDNIGCLYNGAGLAMA TMDLIKHHGGTPANFLDVGGGATVHQVTEA
SucC	EKIILSDKNVKGIFVNIFFGIMKCDVIAEGVIEATKQVGLLELPIVVRLEGTVNELGKKIL
SUCLA2	EKLIITSDKNVLAIVNIFFGIMKCDVIAEGVIEATKQVGLLELPIVVRLEGTVNELGKKIL
SucC	NESGLNIVAAESMADGAQKIVSLV*****
SUCLA2	ADSGKILAGDDLEAARMVVKLSEIVTLAKQAHVDVKFQLP

Fig. 6. (continued)

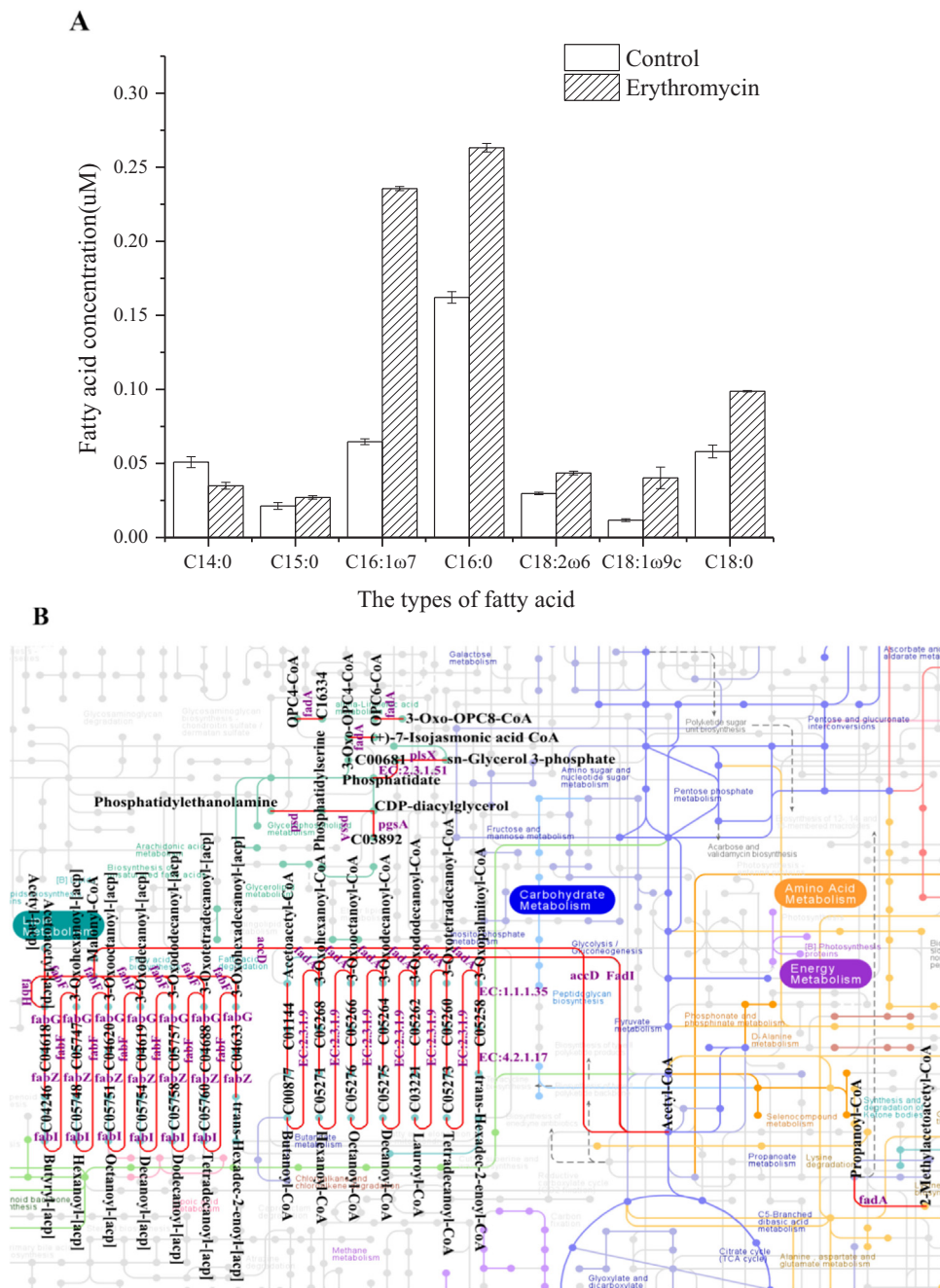


Fig. 7. (A) Fatty acid concentrations of *Bacillus thuringiensis* during the exposure process to erythromycin. The C14:0, C15:0, C16:1ω7, C16:0, C18:2ω6, C18:1ω9c and C18:0 represent myristic acid, pentadecanoic acid, palmitoleic acid, palmitic acid, linoleic/oleic acid, oleic acid and stearic acid, respectively; (B) The network of fatty acid synthesis catalyzed by the functional proteins.

Acknowledgements

The authors would like to thank the National Natural Science Foundation of China (Nos. 21577049 and 41501352), the Science and Technology Project of Guangdong Province (No. 2016A020222005), the Science and Technology Project of Guangzhou City (No. 201707010255) and the Fundamental Research Funds for the Central Universities (No. 21617456) for their financial support.

Appendix A. Supporting information

Supplementary data associated with this article can be found in the online version at <http://dx.doi.org/10.1016/j.ecoenv.2018.05.048>.

References

Blair, J.M.A., et al., 2015. Molecular mechanisms of antibiotic resistance. *Nat. Rev. Microbiol.* 13, 42–51.
 Brar, S.K., et al., 2009. Concurrent degradation of dimethyl phthalate (DMP) during production of *Bacillus thuringiensis* based biopesticides. *J. Hazard. Mater.* 171, 1016–1023.
 Cagliero, C., et al., 2006. Synergy between efflux pump CmeABC and modifications in ribosomal proteins L4 and L22 in conferring macrolide resistance in *Campylobacter jejuni* and *Campylobacter coli*. *Antimicrob. Agents Chemother.* 50, 3893–3896.
 Cai, L., et al., 2011. Acetyl-coA induces cell growth and proliferation by promoting the acetylation of histones at growth genes. *Mol. Cell.* 42, 426–437.
 Canu, A., et al., 2002. Diversity of ribosomal mutations conferring resistance to macrolides, clindamycin, streptogramin, and telitromycin in *Streptococcus pneumoniae*. *Antimicrob. Agents Chemother.* 46, 125–131.
 Carls, A., et al., 2014. Systemic exposure of topical erythromycin in comparison to oral

- administration and the effect on cytochrome P450 3A4 activity. *Br. J. Clin. Pharmacol.* 78, 1433–1440.
- Cetecioglu, Z., et al., 2015. Acute effect of erythromycin on metabolic transformations of volatile fatty acid mixture under anaerobic conditions. *Chemosphere* 124, 129–135.
- Chiappori, F., et al., 2015. DnaK as antibiotic target: hot spot residues analysis for differential inhibition of the bacterial protein in comparison with the human HSP70. *PLoS One* 10. <http://dx.doi.org/10.1371/journal.pone.0124563>.
- Chouchani, C., et al., 2012. First report of *mefA* and *mcrA/mcrB* multidrug efflux pumps associated with *bla*(TEM-1) beta-lactamase in *Enterococcus faecalis*. *Int. J. Infect. Dis.* 16, e104–e109.
- Cockcroft, S., 2009. Phosphatidic acid regulation of phosphatidylinositol 4-phosphate 5-kinases. *Biochim. Biophys. Acta-Mol. Cell Biol. Lipids* 1791, 905–912.
- Dhar, M., et al., 2008. Omega oxidation of 3-hydroxy fatty acids by the human CYP4F gene subfamily enzyme CYP4F11. *J. Lipid Res.* 49, 612–624.
- Dimmock, D., et al., 2010. Quantitative evaluation of the mitochondrial DNA depletion syndrome. *Clin. Chem.* 56, 1119–1127.
- Doyle, S.M., et al., 2015. Interplay between *E. coli* DnaK, ClpB and GrpE during protein disassembly. *J. Mol. Biol.* 427, 312–327.
- Errington, J., 2003. Regulation of endospore formation in *Bacillus subtilis*. *Nat. Rev. Microbiol.* 1, 117–126.
- Fleitas, O., Franco, O.L., 2016. Induced bacterial cross-resistance toward host antimicrobial peptides: a worrying phenomenon. *Front. Microbiol.* 7. <http://dx.doi.org/10.3389/fmicb.2016.00381>.
- Fyfe, C., et al., 2016. Resistance to macrolide antibiotics in public health pathogens. *Cold Spring Harb. Perspect. Med.* 6. <http://dx.doi.org/10.1101/cshperspect.a025395>.
- Gutierrez, M.A., et al., 2016. A novel AhR ligand, 2Al, protects the retina from environmental stress. *Sci. Rep.* 6. <http://dx.doi.org/10.1038/srep29025>.
- Haaber, J., et al., 2016. Bacterial viruses enable their host to acquire antibiotic resistance genes from neighbouring cells. *Nat. Commun.* 7. <http://dx.doi.org/10.1038/ncomms13333>.
- Hove-Jensen, B., et al., 2017. Phosphoribosyl diphosphate (PRPP): biosynthesis, enzymology, utilization, and metabolic significance. *Microbiol. Mol. Biol. Rev.* 81. <http://dx.doi.org/10.1128/MMBR.00040-16>.
- Hove-Jensen, B., McGuire, J.N., 2004. Surface exposed amino acid differences between mesophilic and thermophilic phosphoribosyl diphosphate synthase. *Eur. J. Biochem.* 271, 4526–4533.
- Jiao, L.X., et al., 2015. Heat, acid and cold stresses enhance the expression of DnaK gene in *Alicyclobacillus acidoterrestris*. *Food Res. Int.* 67, 183–192.
- Jung, S.N., et al., 2015. Sugilol inhibits STAT3 activity via regulation of transketolase and ROS-mediated ERK activation in DU145 prostate carcinoma cells. *Biochem. Pharmacol.* 97, 38–50.
- Karim, M.R., et al., 2010. Interaction between chronic arsenic exposure via drinking water and plasma lactate dehydrogenase activity. *Sci. Total Environ.* 409, 278–283.
- Keto-Timonen, R., et al., 2016. Cold shock proteins: a minireview with special emphasis on Csp-family of *Enteropathogenic Yersinia*. *Front. Microbiol.* 7. <http://dx.doi.org/10.3389/fmicb.2016.01151>.
- Kim, H., et al., 2014. Correlation between PDZK1, Cdc37, Akt and breast cancer malignancy: the role of PDZK1 in cell growth through Akt stabilization by increasing and interacting with Cdc37. *Mol. Med.* 20, 270–279.
- Kim, H., et al., 2006. The *Bacillus subtilis* spore coat protein interaction network. *Mol. Microbiol.* 59, 487–502.
- Liu, X.F., et al., 2014. Label-free quantitative proteomics analysis of antibiotic response in *Staphylococcus aureus* to oxacillin. *J. Proteome Res.* 13, 1223–1233.
- Llorca, M., et al., 2015. Identification of new transformation products during enzymatic treatment of tetracycline and erythromycin antibiotics at laboratory scale by an on-line turbulent flow liquid-chromatography coupled to a high resolution mass spectrometer LTQ-Orbitrap. *Chemosphere* 119, 90–98.
- Lobritz, M.A., et al., 2015. Antibiotic efficacy is linked to bacterial cellular respiration. *Proc. Natl. Acad. Sci. USA* 112, 8173–8180.
- Mandal, K., et al., 2013. Microbial degradation of fipronil by *Bacillus thuringiensis*. *Ecotoxicol. Environ. Saf.* 93, 87–92.
- McKenney, P.T., et al., 2013. The *Bacillus subtilis* endospore: assembly and functions of the multilayered coat. *Nat. Rev. Microbiol.* 11, 33–44.
- Mishra, N.N., et al., 2012. Daptomycin resistance in *Enterococci* is associated with distinct alterations of cell membrane phospholipid content. *PLoS One* 7. <http://dx.doi.org/10.1371/journal.pone.0043958>.
- Navratilova, V., et al., 2015. Effect of cholesterol on the structure of membrane-attached cytochrome P450 3A4. *J. Chem. Inf. Model.* 55, 628–635.
- Orlando, R., et al., 2003. Effect of the CYP3A4 inhibitor erythromycin on the pharmacokinetics of lignocaine and its pharmacologically active metabolites in subjects with normal and impaired liver function. *Br. J. Clin. Pharmacol.* 55, 86–93.
- Pal, D., Mitra, A.K., 2006. MDR- and CYP3A4-mediated drug-drug interactions. *J. Neuroimmune Pharmacol.* 1, 323–339.
- Paredes-Sabja, D., et al., 2011. Germination of spores of *Bacillales* and *Clostridiales* species: mechanisms and proteins involved. *Trends Microbiol.* 19, 85–94.
- Penesyan, A., et al., 2015. Antibiotic discovery: combatting bacterial resistance in cells and in biofilm communities. *Molecules* 20, 5286–5298.
- Perez, R.A., et al., 2017. Analysis of macrolide antibiotics in water by magnetic solid-phase extraction and liquid chromatography-tandem mass spectrometry. *J. Pharm. Biomed. Anal.* 146, 79–85.
- Qin, S.S., et al., 2014. Report of ribosomal RNA methylase gene *erm*(B) in multidrug-resistant *Campylobacter coli*. *J. Antimicrob. Chemother.* 69, 964–968.
- Ramamurthi, K.S., Losick, R., 2008. ATP-Driven self-assembly of a morphogenetic protein in *Bacillus subtilis*. *Mol. Cell.* 31, 406–414.
- Reynolds, E., et al., 2003. Msr(A) and related macrolide/streptogramin resistance determinants: incomplete transporters? *Int. J. Antimicrob. Agents* 22, 228–236.
- Roland, K., et al., 2014. Looking for protein expression signatures in European eel peripheral blood mononuclear cells after in vivo exposure to perfluorooctane sulfonate and a real world field study. *Sci. Total Environ.* 468, 958–967.
- Rouabhia, M., et al., 2017. E-cigarette vapor induces an apoptotic response in human gingival epithelial cells through the caspase-3 pathway. *J. Cell. Physiol.* 232, 1539–1547.
- Siibak, T., et al., 2009. Erythromycin- and chloramphenicol-induced ribosomal assembly defects are secondary effects of protein synthesis inhibition. *Antimicrob. Agents Chemother.* 53, 563–571.
- Song, J.Y., et al., 2016. Introduction of a bacterial acetyl-CoA synthesis pathway improves lactic acid production in *Saccharomyces cerevisiae*. *Metab. Eng.* 35, 38–45.
- Strahl, H., Hamoen, L.W., 2010. Membrane potential is important for bacterial cell division. *Proc. Natl. Acad. Sci. USA* 107, 12281–12286.
- Sturm, A., Dworkin, J., 2015. Phenotypic diversity as a mechanism to exit cellular dormancy. *Curr. Biol.* 25, 2272–2277.
- Tang, L.T., et al., 2016. Correlation among phenyltins molecular properties, degradation and cellular influences on *Bacillus thuringiensis* in the presence of biosurfactant. *Biochem. Eng. J.* 105, 71–79.
- Terzic, S., et al., 2018. Biotransformation of macrolide antibiotics using enriched activated sludge culture: kinetics, transformation routes and ecotoxicological evaluation. *J. Hazard. Mater.* 349, 143–152.
- Wang, L.L., et al., 2017. Interactions among triphenyltin degradation, phospholipid synthesis and membrane characteristics of *Bacillus thuringiensis* in the presence of D-malic acid. *Chemosphere* 169, 403–412.
- Yang, M., et al., 2017. Influence of perfluorooctanoic acid on proteomic expression and cell membrane fatty acid of *Escherichia coli*. *Environ. Pollut.* 220, 532–539.
- Yi, W.Y., et al., 2017. Triphenyltin degradation and proteomic response by an engineered *Escherichia coli* expressing cytochrome P450 enzyme. *Ecotoxicol. Environ. Saf.* 137, 29–34.
- Zhang, H., et al., 2016. Glutathionylation of the bacterial Hsp70 chaperone DnaK provides a link between oxidative stress and the heat shock response. *J. Biol. Chem.* 291, 6967–6981.
- Zhang, W.W., et al., 2017. Isolation and characterization of a high-efficiency erythromycin A-degrading *Ochrobactrum* sp strain. *Mar. Pollut. Bull.* 114, 896–902.
- Zhao, Y.L., et al., 2015. Quantitative proteomic analysis of sub-MIC erythromycin inhibiting biofilm formation of *S-suis* in vitro. *J. Proteom.* 116, 1–14.